Helicobacter pylori moves through mucus by reducing mucin viscoelasticity

Jonathan P. Celli[a,1], Bradley S. Turner[b], Nezam H. Afdhal[b], Sarah Keates[b], Ionita Ghiran[b], Ciaran P. Kelly[b], Randy H. Ewoldt[c], Gareth H. McKinley[c], Peter So[d], Shyamsunder Erramilli[a,2], and Rama Bansil[a,2]

[a]Department of Physics, Boston University, Boston, MA 02215; [b]Division of Gastroenterology, Beth Israel Deaconess Medical Center and Harvard Medical School, Boston, MA 02215; and [c]Hatsopoulos Microfluids Laboratory, Department of Mechanical Engineering, and [d]Department of Biological Engineering, Massachusetts Institute of Technology, Cambridge, MA 02139

Edited by Robert H. Austin, Princeton University, Princeton, NJ, and approved July 13, 2009 (received for review March 27, 2009)

The ulcer-causing gastric pathogen *Helicobacter pylori* is the only bacterium known to colonize the harsh acidic environment of the human stomach. *H. pylori* survives in acidic conditions by producing urease, which catalyzes hydrolysis of urea to yield ammonia thus elevating the pH of its environment. However, the manner in which *H. pylori* is able to swim through the viscoelastic mucus gel that coats the stomach wall remains poorly understood. Previous rheology studies on gastric mucin, the key viscoelastic component of gastric mucus, indicate that the rheology of this material is pH dependent, transitioning from a viscous solution at neutral pH to a gel in acidic conditions. Bulk rheology measurements on porcine gastric mucin (PGM) show that pH elevation by *H. pylori* induces a dramatic decrease in viscoelastic moduli. Microscopy studies of the motility of *H. pylori* in gastric mucin at acidic and neutral pH in the absence of urea show that the bacteria swim freely at high pH, and are strongly constrained at low pH. By using two-photon fluorescence microscopy to image the bacterial motility in an initially low pH mucin gel with urea present we show that the gain of translational motility by bacteria is directly correlated with a rise in pH indicated by 2′,7′-Bis-(2-Carboxyethyl)-5-(and-6)-carboxyfluorescein (BCECF), a pH sensitive fluorescent dye. This study indicates that the helicoidal-shaped *H. pylori* does not bore its way through the mucus gel like a screw through a cork as has previously been suggested, but instead achieves motility by altering the rheological properties of its environment.

H. pylori | bacterial motility | rheology | pH | gelation

Helicobacter pylori is a spiral shaped, Gram-negative microorganism, that colonizes the human stomach, a highly acidic environment that is not suitable for any other known microorganism (1–5). It is well known however, that *H. pylori*, which is a neutralophile, is able to survive by producing large amounts of the enzyme urease, which catalyzes hydrolysis of urea present in the stomach to yield NH_3 and CO_2, thus elevating the pH to neutral as necessary for survival (6). It is generally accepted that urea hydrolysis is accomplished by uptake of urea through a proton-gated channel with hydrolysis taking place inside the bacterium and creating a thin neutral layer around the outer surface of the cell (7), although other studies indicate that this crucial enzyme exists on the cell surface (8–10), or that it is secreted or released (11, 12). In addition to its ability to produce urease to elevate pH of its environment, *H. pylori* further protects itself by swimming through the protective layer of gastric mucus in the stomach and attaching to the epithelial cells beneath, where it can cause inflammation over the course of lifelong infection. Both of these factors, the production of urease, and motility, are crucial to the survival of *H. pylori*. Indeed it has been shown that neither urease-deficient mutants (13), nor nonmotile mutants (14) are able to successfully colonize the stomach. However, despite the vital role of motility in *H. pylori* pathogenesis, the actual mechanism by which it achieves motility in the unusual ecological niche of the mucus layer remains poorly understood.

Studies examining the rheological properties of mucus secretions from various mammalian stomachs have established that gastric mucus forms a soft viscoelastic gel, with the elastic component of the frequency-dependent viscoelastic shear modulus, $G'(\omega)$ higher than the viscous component, $G''(\omega)$ over a wide range of oscillatory shear frequencies ω (15–20). Given that the mucus layer exhibits a gel-like rheological response, the question is raised of how a flagellated microorganism such as *H. pylori* is able to swim in such an environment. Although previous studies have examined the motility of *H. pylori* and other bacteria in fluids with varying viscosity (21–25), we are not aware of any experimental studies that indicate the ability of a flagellated prokaryote to swim through a gel with $G'(\omega) > G''(\omega)$. It has been shown however, that gastric mucin, the glycoprotein content of mucus primarily responsible for its viscoelastic response, undergoes a reversible pH-dependent sol-gel transition from a viscous polymer solution to a soft gel as pH is lowered below pH $\approx$ 4, and vice versa as the pH is raised (26, 27). This feature of mucin is believed to play a crucial role in its protective function in the stomach in that by forming a gel at low pH, it forms a viscoelastic barrier protecting the lining of the stomach from damage by its own acidic secretions and other insults (28). Moreover, bicarbonate secretion maintains a gradient from pH 2 in the gastric lumen to approximately neutral pH at the epithelial surface (29, 30). *H. pylori*, has been shown to exhibit a pH tactic response toward elevated pH (31), consistent with the established picture of a bacterium swimming through the mucus layer toward the epithelial surface and away from the highly acidic lumen. However, this tropism still does not explain the manner in which it is motile at all in the low pH mucin gel. In this study we propose to combine the knowledge of the pH-dependent rheological properties of mucin, with the pH-elevation by *H. pylori* to provide an explanation of how this bacterium is motile in the mucus layer. The fundamental hypothesis of this study is that *H. pylori* does not generate sufficient motor torque to be able to propel itself through a viscoelastic mucus gel in the absence of a means to modify mucus viscoelasticity. However, the urease induced pH elevation of *H. pylori* triggers the transition from gel to sol of gastric mucin and enables the bacteria, which would otherwise be immobile, to swim freely through the mucus.

Author contributions: J.P.C., G.H.M., P.S., S.E., and R.B. designed research; J.P.C., B.S.T., P.S., and R.B. performed research; J.P.C., B.S.T., N.H.A., S.K., I.G., C.P.K., R.H.E., P.S., S.E., and R.B. contributed new reagents/analytic tools; J.P.C., R.H.E., S.E., and R.B. analyzed data; and J.P.C., S.E., and R.B. wrote the paper.

The authors declare no conflict of interest.

This article is a PNAS Direct Submission.

[1]Present address: Wellman Center for Photomedicine, Massachusetts General Hospital and Harvard Medical School, Boston, MA 02114.

[2]To whom correspondence may be addressed. E-mail: shyam@bu.edu or rb@bu.edu.

This article contains supporting information online at www.pnas.org/cgi/content/full/0903438106/DCSupplemental.

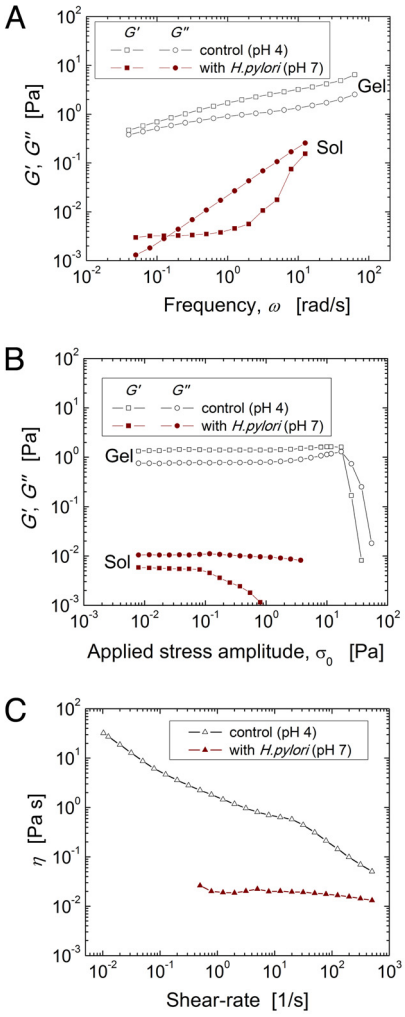

Fig. 1. Porcine gastric mucin (PGM) viscoelasticity decreases dramatically when incubated with *H. pylori* concomitant with measured elevation in pH. Two PGM samples are initially prepared to pH 4; one is kept as a control sample (open symbols) and the other is incubated with *H. pylori* (closed symbols) which neutralizes the sample to pH 7. (*A*) Frequency dependent linear viscoelastic moduli, G′ (squares) and G′′ (circles) (*B*) Nonlinear dependence of viscoelastic moduli on applied oscillatory shear stress (constant frequency, ω = 0.5 rad/s) (*C*) Steady shear viscosity as a function of shear-rate.

Results

***H. Pylori* Elevates pH and Reduces Bulk Vscoelasticity in Gastric Mucin.** To test the hypothesis that the pH-elevation caused by *H. pylori* urease activity impacts mucin viscoelasticity, we compared the rheological response of porcine gastric mucin (PGM) with and without *H. pylori* present. Samples were prepared with artificial gastric juice containing urea and hydrochloric acid driving the initial pH to 4. Although pH remained constant in control samples over the period of incubation, in the presence of *H. pylori*, the pH rapidly elevated to 7.1 to 7.4. In addition to the measured change in pH, we found that there was also a profound difference in the rheological response of the two samples in a manner that was strikingly consistent with that observed in the pH 4 (gel) and pH 6 (solution) buffered PGM samples previously published (26). Frequency dependent viscoelastic moduli (Fig. 1*A*) exhibit a dramatic drop in the values of both $G'(\omega)$ and $G''(\omega)$ and a change from storage dominant to loss dominant response indicative of the transition from gel to solution in the sample with bacteria present, in direct parallel with the difference between pH 4 and pH 6 buffered samples previously observed. Because of the dramatic loss of elasticity concomitant with the pH elevation in PGM incubated with *H. pylori*, values of $G'(\omega)$ are approaching the limits of sensitivity of the rheometer, and hence should be treated as approximate measurements. Measurements of the nonlinear viscoelastic response of each sample (Fig. 1*B*), reveal the characteristic yield stress and "weak strain overshoot" as described by Hyun et al. (32), in the control sample. However, this behavior has completely vanished in the sample with *H. pylori* which, like the previously published pH 6 (solution) sample, has a very limited linear response regime below 0.1 Pa (26). Finally, the dramatic loss of viscosity and diminishing of shear thinning behavior because of *H. pylori* observed in steady shear experiments (Fig. 1*C*) is also consistent with analogous tests on buffered samples. The degradation in viscoelasticity of PGM in the presence of *H. pylori* observed here is consistent with the measured change in pH produced by the bacteria in every rheology test examined.

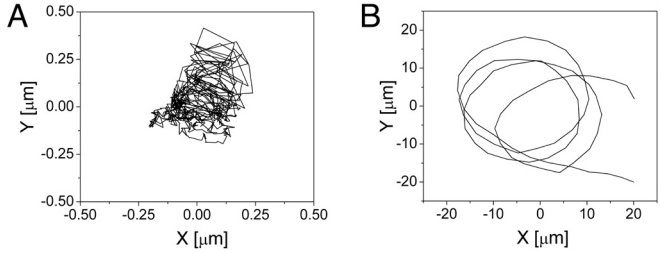

Fig. 2. Representative trajectories for bacteria in PGM gel (*A*) and solution (*B*) obtained by particle tracking. Note the dramatically smaller scale on the axes in *A*, where *H. pylori* are confined in the mucin gel, whereas in the mucin solution bacteria move freely about the field of view in large arcing trajectories.

***H. pylori* Is Highly Motile in Gastric Mucin Solution, While Confined in Gel.** Further studies were conducted to examine the motility of *H. pylori* in PGM solution (pH 6) and gel (pH 4), without urea present (Movie S1 and Movie S2).. At pH 6 bacteria were observed to swim freely, typically moving in circular trajectories with radii on the order of 20 μm as shown in Fig. 2*A*. By using particle tracking methods it was possible to analyze several representative trajectories from image sequences to calculate a swimming speed (previously described as curvilinear velocity (33)) to be 27 $\pm$ 5 μm/s. In contrast, bacteria in the gel phase PGM were clearly elastically confined, undergoing displacements on the order of hundreds of nanometers only (Fig. 2*B*), despite the fact that high resolution (100X) images of single cells shown in Fig. 3 exhibited rapid rotation of the helical flagella bundle and non-Brownian driven oscillations of the body. The circular trajectories consistently observed in PGM solution could be a surface effect because of swimming close to the solid boundaries of the microscope slide or coverslip. This near surface swimming has been established to give rise to circular motion (34) with fluctuations in the radius of curvature driven by amplified coupling of Brownian

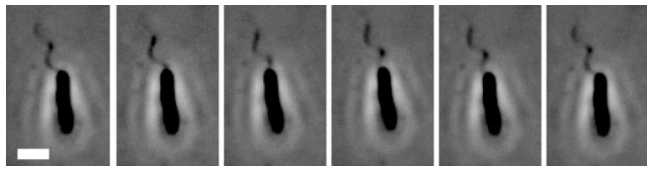

Fig. 3. Snapshots from a time resolved sequence of 100X phase contrast microscopy images of a single *H. pylori* bacterium embedded in PGM gel illustrating flagella rotation from frame to frame. Consecutive images from *Left* to *Right* are separated by 70 ms time intervals. Scale bar, 2 μm.

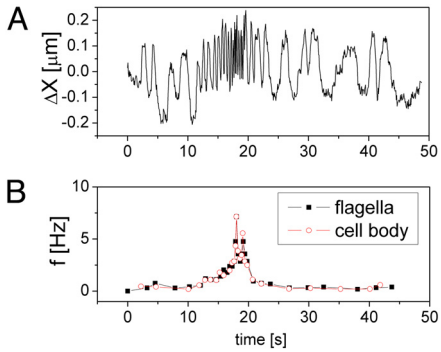

Fig. 4. Time dependent displacement and frequency data for a confined bacterium. (*A*) Displacement perpendicular to the long axis of the cell body as a function of time for a single bacterium trapped in mucin gel determined by tracking the centroid in consecutive frames. (*B*) Frequency of oscillations for the same bacterium calculated from cell body displacements above and determined by manually counting flagella rotation cycles.

motion with hydrodynamic interactions (35). It is interesting to note that in PGM solution, *H. pylori* were observed to undergo long continuous runs punctuated only by occasional brief tumbling events, while in a previous study pronounced run and tumble behavior was observed in (nonmucin) solution (33). In the present study, however, the emphasis is placed on the mechanism underlying the profound disparity in motility observed between *H. pylori* in mucin solution versus mucin gel.

Analysis of the sequences of images obtained at 100X facilitated measurement of morphological parameters of the flagella bundle and dynamics of the bacterial cell body in this confined situation. Several consecutive frames from a movie of the μm scale motion of a confined bacterium are shown (Fig. 3). From these images, the helical pitch, p, and radius, r, of the flagella bundle were measured to be 2.1 μm and 0.57 μm, respectively, and the length, L, of the flagella to be 3.2 μm. Although the individual filaments, of 20–25 nm in diameter (36, 37), that comprise the polar flagella bundle are challenging to image, the bundle of 4–6 filaments is clearly discernible (Fig. 3). The actual thickness cannot be reliably measured by optical microscopy, but assuming 6 filaments come together in a tightly packed tubular geometry (one flagellum in the center surrounded by 5 flagella) we estimate that the diameter is ≈2.71 times that of a single filament, or ≈ 60 nm, which is the value of this parameter used in calculations below.

During the time of observation of the bacterium for which snapshots are shown (Fig. 3 and Movie S1), both the cell body and flagella bundle initially oscillated at a low frequency but later accelerated dramatically to a peak value before slowing down again. Analyzing the time dependent motion in this sequence it was possible to measure the frequency as a function of time for both the counterrotation of the cell body, measured by particle tracking, and the flagella bundle itself. As seen in Fig. 4, there is a 1:1 correlation, indicating that the oscillations of the cell body, which are in fact two dimensional projections of the rotation of the curved asymmetric cell body shape, are purely driven by rotation of the flagella in combination with the restoring force of the medium. The abrupt rise and fall seen in the rotation rate data, suggests that perhaps the cell struggles to set itself free in response to its mechanical confinement, but further studies are warranted to examine the biochemical mechanisms underlying these fluctuations. For example, it is unclear whether this behavior is caused by a local spatial variation in chemoattractant concentration driving the motor to turn more rapidly, or if fluctuations in local shear rate are part of a passive modification of the material properties of the bacterium's non-Newtonian environment as discussed in a recent study on locomotion in a viscoelastic environment (38). This behavior was typical among cells imaged in pH 4 PGM.

Flagella and cell body frequency data can each be independently used to solve for motor torque by the methods of Magariyama et al. (39–41):

$$T_m = \beta_c \omega_c$$

where ω_c is the rotation rate of the cell body (measured above), and β_c is the rotational drag coefficient of the cell body (which is assumed to be a prolate ellipsoid with width 2a and length 2b in a liquid of viscosity η) and is given by:

$$\beta_c = 8\pi\eta a^3 \left[1 - \frac{3}{5}\left(1 - \frac{b}{a}\right)\right]$$

Alternatively, a similar expression can be written for the motor torque for flagella rotation information in terms of the rotation rate of the flagella, ω_f, the flagella rotational drag coefficient, β_f, the translational velocity of the cell body, v_c, and a factor for the ratio of the propulsive force to the rotation rate of the flagella, γ_f:

$$T_m - \beta_f \omega_f - \gamma_f v_f$$

In the present experiments, bacteria are stuck, so $v_c = 0$ and the second term vanishes (hence it is superfluous to define the factor γ_f here). The rotational drag coefficient of the flagella is given in terms of the viscosity of the fluid and the pitch, p, radius, r, length, L and cross sectional diameter, 2d of the flagella by:

$$\beta_f = \frac{2\pi\eta L}{[\ln(2p/d) - 1/2](4\pi^2 r^2 + p^2)}(4\pi^2 r^2 + 2p^2)r^2$$

Using an estimate of $\eta \approx 1$ Pa-s (Fig. 1*C*), and experimental measurements of $a = 0.45$ μm and $b = 2.15$ μm in Eq. **2**, gives $\beta_c = 7.5 \times 10^{-18}$ N m s rad^{-1}. Inserting this value, and the frequency data above in Eq. **1** yields an average torque value of 1.4×10^{-17} N m, with a peak torque at the maximum rotation rate of 5.3×10^{-17} N m. Conducting the independent calculation of motor torque from Eq. **3** (where in this case, $\omega_c = \omega_f$ from Fig. 4) and using the geometrical factors for the flagella quoted above in Eq. **4** yields an average motor torque of 3.6×10^{-18} N m and a peak torque for the times probed of 1.3×10^{-17} N m. It is generally agreed that the calculation of motor torque from the flagella rotation data are more robust because the flagella geometry is well described as a helix whereas the modeling of cell body shape requires somewhat more of an idealization. Nevertheless, the independently derived values here are within a factor of three. In either case, these torque calculations should be treated as rough estimates given that the hydrodynamic drag formulae above do not account for many aspects of the behavior of gastric mucin described in ref. 26, including elasticity, shear thinning, and nonlinear response above a yield stress of ≈10 Pa.

In the Presence of Urea, *H. pylori* Elevate pH of Mucin Gel to Swim Freely. Finally, to tie together the observations from the rheology studies and the preliminary motility studies described above, we observed the motility of bacteria that were added to PGM samples with an initial pH of ≈2, and in the presence of a 5 mM urea concentration. Although initially confined by the gel as discussed above, after ≈30-min bacteria were swimming as if in pH 6 PGM. To reinforce this observation, we conducted two-photon fluorescence imaging of PGM with *H. pylori* in the presence of the pH-sensitive dye, BCECF, which increases in fluorescence emission as pH rises from acidic to neutral, allowing for direct observation of the pH elevation while observing the bacteria themselves. The washed bacteria were

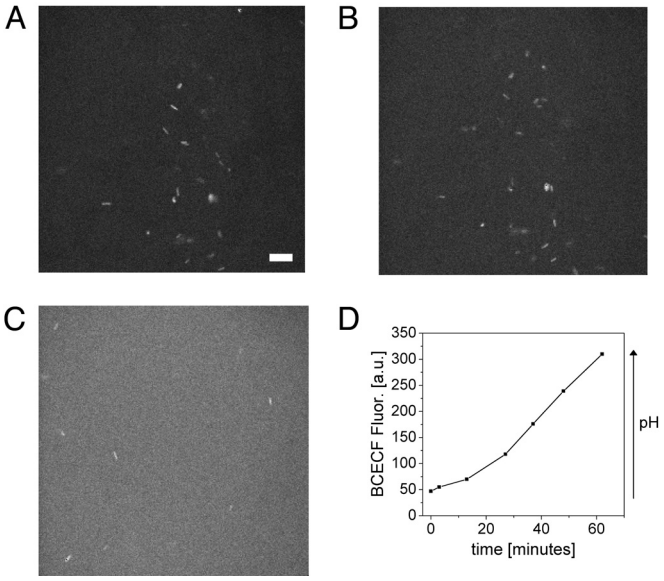

Fig. 5. Two-photon fluorescence imaging of H. pylori in PGM. *H pylori* (stained with BacLight) in PGM with 5 mM urea, prepared with BCECF and driven to an initial pH of 2 by HCl (*A*), immediately after sample preparation (Scale bar, 10 μm) (*B*), at 3 min following preparation, and (*C*), at 27 min following preparation. A plot of the corresponding rise in BCECF fluorescence intensity over time is shown in *D*.

also separately labeled using BacLight (Invitrogen), a fluorescent dye to stain bacterial cells so that the cells could be imaged separately from the fluorescence background. The narrow depth of focus made possible by the use of two-photon fluorescence excitation from a high speed laser scanning source facilitated imaging bacteria without washout from out-of-plane BCECF fluorescence. The use of two-photon excitation also allowed for extended duration live cell imaging of *H. pylori* as illumination of the specimen was accomplished with near infrared light, avoiding photodestruction because of blue light activation of porphyrins known to accumulate in this microorganism (42). In Fig. 5, three representative frames from this sequence of images of bacteria in a PGM gel initially at pH 2 are shown. After 3 min (Fig. 5*B*) the bacteria, which appear as bright spots against the initially nonfluorescent background are still embedded in their initial positions. However, after 27 min (Fig. 5*C*) there has been a significant increase in pH as shown by the increase in fluorescence, and correlated with the increased motility of the bacteria which have begun swimming and are clearly in different positions in the images. In Fig. 5*D* overall BCECF intensity, as determined by taking the average pixel values from regions of images free of bacteria, is plotted against time. The kinetics were found to vary slightly in samples with varying initial pH values, but always exhibited the same qualitative behavior with a monotonic rise in fluorescence intensity in correspondence with the pH elevation. This observation is consistent with previous studies on the kinetic properties of *H. pylori* urease (43).

Discussion

The central result of this study, summarized schematically in Fig. S1 , indicates that pH elevation by *H. pylori*, long known to be vital to its very survival in the stomach, also facilitates the mechanism by which this microorganism is able to achieve motility in the mucus layer. By hydrolysis of urea to elevate the pH of its environment, *H. pylori* reduces viscoelasticity in the mucin gel, thus modifying the environment in which it is initially elastically confined and unable to translate. To do this it creates the conditions of a neutral pH PGM solution in which it is able to swim freely to penetrate the mucus layer and attach to epithelial cells. By extension, this dramatic reduction in the viscoelasticity of mucin via pH elevation from urea hydrolysis may also be important to understanding how *H. pylori* impacts the integrity of the mucus layer compromising its role as a protective viscoelastic barrier. Taken together this presents a picture of a dynamic system in which the bacterium directly influences the rheological properties of the host mucus, which in turn determines the motility of the bacterium.

It is worth noting that the impact of the bacteria on mucin rheology presented here may in fact be the combined result of the pH dependent effects discussed here, and possible proteolytic digestion of PGM because of other enzymes produced by *H. pylori*. Indeed the breakdown of gastric mucin by *H. pylori* has been previously examined by others, but with apparently contradictory results. Early in vitro studies suggest that *H. pylori* directly compromises the mucus layer by proteolytic degradation of mucin glycoproteins (44, 45). In later studies however, other researchers conclude that an observed loss of high particle weight glycoprotein in mucus from ulcer patients is not the result of proteolytic enzymes, but perhaps from a carbonate-bicarbonate buffer at the mucosal surface because of the hydrolysis of urea (46). In another study comparing biopsy samples from patients with and without *H. pylori* infection, one group concludes that although *H. pylori* causes structural changes in the mucus layer in vivo, it does not cause a major overall compromise of the barrier (47). Finally, in studies by another group comparing the viscosity of mucus from a small group of infected patients, untreated subjects, and those after eradication, it is contested that *H. pylori* infection does not reduce the viscosity of gastric mucus (48). However, given the strong correlation with the sharp rise in pH in the presence of *H. pylori* and the subsequent change in rheology in nearly exact parallel with the pH dependence of every measure of viscoelastic response previously established (26), the results here indicate that the dominant effect of *H. pylori* on gastric mucin rheology is that due to pH elevation. Small differences in moduli are related to use of HCl which leads to different ionic strength than the buffers used in previous studies (26, 49, 50).

In this study the fact that bacteria are physically trapped by the mucin gel provided us with an interesting opportunity to examine their dynamics and facilitated calculation of motor torque by two independent methods. To examine the magnitude of the best estimate of torque of 3.6×10^{-18} N m in relation to the yield stress of gastric mucin, one can divide the torque by the approximate swept volume of the flagella, $V = \pi r^2 L = 3.2\ \mu m^3$, to obtain a stress of ≈ 1 Pa. This indicates that the magnitude of torque exerted here is within the linear response regime of the mucin gel. Further microrheology studies examining the breakdown of the linear response regime of mucin gels are warranted to determine if the material would yield at the same stress on the μm length scales probed here, as in the bulk.

Using the flagella frequency derived value as the basis for comparison, this average torque of 3.6×10^{-18} N m is approximately an order of magnitude higher than measurements by Li and Tang for *Caulobacter Crescentus* (3.5×10^{-19} N m) (51), and approximately a factor of three higher than torque measured by Reid et al. for *E. Coli* (1.3×10^{-18} N m) (52). This is consistent with Li and Tang's hypothesis that the low motor torque and high swimming efficiency of *C. Crescentus* are necessary for survival in the extremely nutrient-poor fresh water environments it has adapted to survive in. In contrast, *E. Coli* and *H. pylori* inhabit the nutrient rich human gut and do not require efficiency of flagella rotation for survival. In the case of *H. pylori*, the generation of an extremely high torque may be important to twist the flagella hard enough to move through mucin at moderately low pH values.

It is interesting to note that the pH elevation observed in the fluorescent images in this study does not appear to be a local effect in the immediate vicinity of a given bacterium, but rather a global effect over the entire sample. This widespread pH elevation was likely caused by the rapid diffusion of NH_3 molecules produced from urea hydrolysis because of each bacterium. With an estimated diffusion constant of $D \approx 10^{-9}$ m^2/s, NH_3 initially in the vicinity of each bacterium would diffuse the ≈ 20 μm radial separation to the next cell in less than $\approx$ 70 ms thus continuously driving up the pH of the entire specimen. However, this in vitro model system does not reflect the full dynamics of the mucus layer in vivo, in which the temporal-spatial pH profile is influenced by continuous secretion of hydrochloric acid and bicarbonate in addition to the activity of the *H. pylori* urease. It was also noted in these images that the bacteria themselves became brighter as time went on suggesting that some of the BCECF passes through the cell wall into the interior of the bacterium. This observation may be consistent with the periplasmic pH elevation reported by Athmann et al. in confocal microscopy studies (53).

Our finding that *H. pylori* achieves motility by altering the rheological properties of its environment, challenges the previously suggested explanation that *H. pylori* simply bores its way through the mucus gel like a corkscrew (5). As shown in our study, *H. pylori*, albeit an adept swimmer, does not generate sufficient torque to swim through a gel. Instead, it achieves motility by modifying the rheology of its environment, a feat that is facilitated by coupling of the pH-dependent rheology of gastric mucin and pH-elevation driven by urease mediated urea hydrolysis. Observations made in the course of this study, which examines the unusual situation of a bacterium apparently struggling against elastic confinement, raise additional questions, for example: Are rotations of the helicoidal cell body important to translational motility, or merely incidental to the flagella rotations? What causes abrupt fluctuations in rotation frequency of the confined bacterium? Is this purely a biochemical response or could this be part of a feedback system by which the bacterium interacts with the frequency dependent mechanical properties of its environment? Also, while providing an explanation of the manner in which this microorganism overcomes the physical constraints imposed by its environment, we raise the broader question pertaining to motility in a viscoelastic medium, a problem which is in general, poorly understood. Theoretical studies similar to the recent work on sperm motility in a viscoelastic media (54) would be invaluable to improve our understanding of motility in relation to medium viscoelasticity for swimmers such as *H. pylori*, for which the helical flagella bundle is driven by a rotary motion (rather than the whip-like motion that propels sperm). In general, a more complete theoretical understanding of the full frequency dependent nonlinear response of the medium to the motion of the flagella and cell body is required to better understand the motility of *H. pylori* and other flagellated prokaryotes in physiologically relevant conditions. Furthermore, understanding the motility of bacteria swimming through gels is of relevance to many other situations where bacteria infect gels, for example food products, and hydrogels used as tissue scaffolds and biofilms.

Methods

***H. Pylori* Culture.** ATCC strain 43504 *H. pylori* from frozen glycerol stocks (−80 °C) were first streaked onto *Brucella* agar, supplemented with 5% horse blood (BBL, Becton Dickinson Microbiology) and then incubated at 37 °C under microaerophillic conditions containing 5%–12% CO_2 and 5%–15% O_2 for 24 h. After initial culture on blood agar plates, bacteria were then rinsed into a liquid culture media consisting of brain heart infusion and other nutrients, and subsequently cultured in liquid broth for an additional 24–48 h under constant gentle agitation at 90 rpm. Bacteria were removed from culture for study during the exponential phase of growth, washed, then resuspended in PBS (PBS). *H. pylori* were grown to an optical density of 1.0 at 600 nm.

Mucin Sample Preparation. In this work Porcine Gastric Mucin (PGM) was used as a model system for human gastric mucin. PGM was obtained from pig stomachs and purified by Sepharose CL-2B column chromatography and density gradient ultracentrifugation as described in ref. 27. Samples for rheology were prepared to the appropriate pH using an artificial gastric juice preparation as previously described (55) (but modified to include only hydrochloric acid without additional salts, and in some samples, urea) and left to equilibrate for 48 h before study. The final concentration of PGM with artificial gastric juice and *H. pylori* solution was 15 mg/ml. Changes in pH were measured using a pH electrode in solution before placing the mucin preparation on the microscope slide.

Rheology Studies. Rheological data were obtained using a TA instruments AR-2000 stress-controlled rheometer. Typically 400 μl of sample was available for study and the gap height was set to sufficiently fill the area of the 40-mm plate, usually 200–300 μm. Following initial calibration for instrument inertia and parallel plate geometry inertia, stress sweeps at constant frequency were performed to establish the regime of linear response for each sample, i.e., the region in which the applied shear stress is linearly proportional to the strain. A constant stress in the identified linear regime was then used to conduct the subsequent frequency sweep, creep test (step stress), and flow test (steady shear) on the sample.

Microscopy and Imaging. *H. pylori* were imaged on an Olympus IX-70 inverted microscope using 20X and 100X objectives. Samples were prepared for imaging on standard glass microscope slides and cover slips sealed with Secure-Seal 0.12 mm imaging spacers (Sigma–Aldrich). Images of freely swimming bacteria were obtained at 20X using phase contrast or dark-field microscopy, while 100X A Qicam cooled monochrome CCD camera (Qimaging) mounted on the microscope was used to obtain sequences of digital images in the multipaged TIFF format. Image sequences were analyzed in IDL software to identify individual bacteria coordinates and link these together frame by frame to form trajectories using particle tracking methods previously described by others (56, 57).

Two-Photon Fluorescence Microscopy. Two-photon fluorescence images were obtained with a 40X objective using 800 nm excitation light from a pulsed laser source (a Tsunami Ti:Sapphire laser pumped by a 5W Millenia, Spectra Physics) at a power of 100 mW. This illumination produced an excitation volume with full width at half maximum of 0.3 μm in the radial direction and 0.9 μm in the axial direction. Images were obtained with a scan rate of 5 kHz. As described in the text fluorescence contrast was generated using BacLight (Invitrogen) and 2′,7′-Bis-(2-Carboxyethyl)-5-(and-6)-carboxyfluorescein (BCECF) (Invitrogen) following manufacturers guidelines, to image the bacterial cells and the pH change in the surrounding mucin.

ACKNOWLEDGMENTS. We thank Professors Anders Sandvik, Sidney Redner, and Bernard Chasan of the Department of Physics at Boston University for valuable conversations about this work and R.E. Goldstein for advice and discussions. This work supported by National Institutes of Health Grant KO1-DK075942 (to S.K.); American Gastroenterological Association, Foundation for Digestive Health and Nutrition TAP Endowed Designated Research Award in Acid Related Diseases; Intergovernmental Personnel Act Assignment at the National Science Foundation (NSF) Independent Research and Development (IRD) (R.B.); and the National Science Foundation GK12 Graduate Fellowship (J.C.).

1. Blaser MJ (1996) The bacteria behind ulcers. *Sci Am* 274(2):104–107.
2. Blaser MJ (2005) An endangered species in the stomach. *Sci Am* 292(2):38–45.
3. Marshall BJ, Langton SR (1986) Urea hydrolysis in patients with *Campylobacter pyloridis* infection. *Lancet* 1:965–966.
4. Marshall BJ, Warren JR (1984) Unidentified curved bacilli in the stomach of patients with gastritis and peptic ulceration. *Lancet* 1:1311–1315.
5. Montecucco C, Rappuoli R (2001) Living dangerously: How *Helicobacter pylori* survives in the human stomach. *Nat Rev Mol Cell Biol* 2:457–466.
6. Mobley HL, Cortesia MJ, Rosenthal LE, Jones BD (1988) Characterization of urease from *Campylobacter pylori*. *J Clin Microbiol* 26:831–836.
7. Weeks DL, Eskandari S, Scott DR, Sachs G (2000) A H+-gated urea channel:The link between *Helicobacter pylori* urease and gastric colonization. *Science* 287:482–485.
8. Baik SC et al. (2004) Proteomic analysis of the sarcosine-insoluble outer membrane fraction of *Helicobacter pylori* strain 26695. *J Bacteriol* 186:949–955.
9. Dunn BE, Phadnis SH (1998) Structure, function and localization of *Helicobacter pylori* urease. *Yale J Biol Med* 71(2):63–73.
10. Phadnis S, et al. (1996) Surface localization of *Helicobacter pylori* urease and a heat shock protein homolog requires bacterial autolysis. *Infect Immun* 64:905–912.
11. Gobert AP, et al. (2002) Cutting edge: Urease release by *Helicobacter pylori* stimulates macrophage inducible nitric oxide synthase. *J Immunol* 168:6002–6006.
12. Vanet A, Labigne A (1998) Evidence for specific secretion rather than autolysis in the release of some *Helicobacter pylori* proteins. *Infect Immun* 66:1023–1027.
13. Eaton KA, Brooks CL, Morgan DR, Krakowka S (1991) Essential role of urease in pathogenesis of gastritis induced by *Helicobacter pylori* in gnotobiotic piglets. *Infect Immun* 59:2470–2475.
14. Eaton K, Morgan D, Krakowka S (1992) Motility as a factor in the colonisation of gnotobiotic piglets by *Helicobacter pylori*. *J Med Microbiol* 37:123–127.
15. Allen A, Bell A, Mantle M, Pearson JP (1982) The structure and physiology of gastrointestinal mucus. *Adv Exp Med Biol* 144:115–133.
16. Bell AE, Allen A, Morris E, Rees DA (1982) Rheological studies on native pig gastric mucus gel. *Adv Ex Med Biol* 144:97–99.
17. Bell AE, et al. (1985) Properties of gastric and duodenal mucus: Effect of proteolysis, disulfide reduction, bile, acid, ethanol, and hypertonicity on mucus gel structure. *Gastroenterology* 88:269–280.
18. Sellers LA, Allen A (1989) Gastrointestinal mucus gel rheology. *Symp Soc Exp Biol* 43:65–71.
19. Sellers LA, Allen A, Morris ER, Ross-Murphy SB (1987) Mechanical characterization and properties of gastrointestinal mucus gel. *Biorheology* 24:615–623.
20. Sellers LA, Allen A, Morris ER, Ross-Murphy SB (1991) The rheology of pig small intestinal and colonic mucus: Weakening of gel structure by non-mucin components. *Biochim Biophys Acta* 1115:174–179.
21. Schneider WR, Doetsch RN (1974) Effect of viscosity on bacterial motility. *J Bacteriol* 117:696.
22. Suzuki H, Kurabayashi K, Hibi T (2005) [*H. pylori* motility analysis]. *Nippon Rinsho 63 Suppl* 11:209–212.
23. Worku ML, et al. (1999) Motility of *Helicobacter pylori* in a viscous environment. *Eur J Gastroenterol Hepatol* 11:1143–1150.
24. Yoshiyama H, Nakamura H, Kimoto M, Okita K, Nakazawa T (1999) Chemotaxis and motility of *Helicobacter pylori* in a viscous environment. *J Gastroenterol 34 Suppl* 11:18–23.
25. Berg HC, Turner L (1979) Movement of microorganisms in viscous environments. *Nature* 278:349–351.
26. Celli JP, et al. (2007) Rheology of gastric mucin exhibits a pH-dependent sol-gel transition. *Biomacromolecules* 8(5):1580–1586.
27. Cao X, et al. (1999) pH-dependent conformational change of gastric mucin leads to sol-gel transition. *Biophys J* 76:1250–1258.
28. Bhaskar KR, et al. (1992) Viscous fingering of HCl through gastric mucin. *Nature* 360:458–461.
29. Allen A (1981) Structure and function of gastrointestinal mucus. *Physiology of the gastroenterology tract*, ed Johnson L (Raven Press, New York, NY), 1st Ed, pp 617–639.
30. Allen A, Flemstrom G (2005) Gastroduodenal mucus bicarbonate barrier: Protection against acid and pepsin. *Am J Physiol* 288:C1–19.
31. Croxen MA, Sisson G, Melano R, Hoffman PS (2006) The *Helicobacter pylori* chemotaxis receptor TlpB (HP0103) is required for pH taxis and for colonization of the gastric mucosa. *J Bacteriol* 188:2656–2665.
32. Hyun K, Kim S, Ahn K, Lee S Large amplitude oscillatory shear as a way to classify the complex fluids. *J Non-Newton Fluid* 107:51–65, 2002.
33. Karim QN, Logan RP, Puels J, Karnholz A, Worku ML (1998) Measurement of motility of *Helicobacter pylori*, *Campylobacter jejuni*, and *Escherichia coli* by real time computer tracking using the Hobson BacTracker. *J Clin Pathol* 51:623–628.
34. Lauga E, DiLuzio WR, Whitesides GM, Stone HA (2006) Swimming in circles: Motion of bacteria near solid boundaries. *Biophys J* 90:400–412.
35. Li G, Tam L-K, Tang JX (2008) Amplified effect of Brownian motion in bacterial near-surface swimming. *Proc Natl Acad Sci USA* 105:18355–18359.
36. O'Rourke J, Bode G (2001) Morphology and Ultrastructure. *Helicobacter pylori*: *Physiology and Genetics*, eds Mobley H, Mendz G (ASM Press, Washington DC), pp 53–67.
37. Worku ML, Sidebotham RL, Walker MM, Keshavarz T, Karim QN (1999) The relationship between *Helicobacter pylori* motility, morphology and phase of growth: Implications for gastric colonization and pathology. *Microbiology* 145:2803–2811.
38. Lauga E (2007) Propulsion in a viscoelastic fluid. *Phys Fluids* 19:083104.
39. Magariyama Y, Kudo S (2002) A mathematical explanation of an increase in bacterial swimming speed with viscosity in linear-polymer solutions. *Biophys J* 83:733–739.
40. Magariyama Y, Sugiyama S, Kudo S (2001) Bacterial swimming speed and rotation rate of bundled flagella. *FEMS Microbiol Lett* 199:125–129.
41. Magariyama Y, et al. (1995) Simultaneous measurement of bacterial flagellar rotation rate and swimming speed. *Biophys J* 69:2154–2162.
42. Hamblin MR, et al. (2005) *Helicobacter pylori* accumulates photoactive porphyrins and is killed by visible light. *Antimicrob Agents Chemother* 49:2822–2827.
43. Cesareo SD, Langton SR (1992) Kinetic properties of Helicobacter pylori urease compared with jack bean urease. *FEMS Microbiol Lett* 78(1):15–21.
44. Slomiany BL, et al. (1987) *Campylobacter pyloridis* degrades mucin and undermines gastric mucosal integrity. *Biochem Biophys Res Commun* 144:307–314.
45. Slomiany BL, Sarosiek J, Bilski J, Slomiany A (1988) Evidence for proteolytic disruption of gastric mucus coat by *Campylobacter pylori*. *S Afr Med J* 74:40–41.
46. Sidebotham RL, Batten JJ, Karim QN, Spencer J, Baron JH (1991) Breakdown of gastric mucus in presence of *Helicobacter pylori*. *J Clin Pathol* 44:52–57.
47. Newton JL, et al. (1998) *Helicobacter pylori* in vivo causes structural changes in the adherent gastric mucus layer but barrier thickness is not compromised. *Gut* 43:470–475.
48. Markesich DC, Anand BS, Lew GM, Graham DY (1995) Helicobacter pylori infection does not reduce the viscosity of human gastric mucus gel. *Gut* 36:327–329.
49. Snary D, Allen A, Pain RH (1971) The structure of pig gastric mucus. Conformational transitions induced by salt. *Eur J Biochem* 24:183–189.
50. Waigh T, et al. (2002) Entanglement coupling in porcine stomach mucin. *Langmuir* 18:7188–7195.
51. Li G, Tang JX (2006) Low flagellar motor torque and high swimming efficiency of Caulobacter crescentus swarmer cells. *Biophys J* 91:2726–2734.
52. Reid SW, Leake MC, Chandler JH, Lo C, Armitage JP (2006) The maximum number of torque-generating units in the flagellar motor of *Escherichia Coli* is at least 11. *Proc Natl Acad Sci USA* 103:8066–8071.
53. Athmann C, et al. (2000) Local pH elevation mediated by the intrabacterial urease of *Helicobacter pylori* cocultured with gastric cells. *J Clin Invest* 106:339–347.
54. Fu HC, Powers TR, Wolgemuth CW (2007) Theory of swimming filaments in viscoelastic media. *Phys Rev Lett* 99:258101.
55. Bhaskar KR, et al. (1991) Profound increase in viscosity and aggregation of pig gastric mucin at low pH. *Am J Physiol* 261:G827–832.
56. Crocker J, Grier D (1996) Methods of digital video microscopy for colloidal studies. *J Colloid Interface Sci* 179:298–313.
57. Mason TG, Ganesan K, van Zanten JH, Wirtz D, Kuo SC (1997) Particle tracking microrheology of complex fluids. *Phys Rev Lett* 79:3282.